Pharmaceutical Research, Vol. 26, No. 1, January 2009 (© 2008)
DOI: 10.1007/s11095-008-9710-4

Research Paper

Poly (lactide-*co*-glycolide)-Polymethacrylate Nanoparticles for Intramuscular Delivery of Plasmid Encoding Interleukin-10 to Prevent Autoimmune Diabetes in Mice

Ashwin Basarkar[1] and Jagdish Singh[1,2]

Received April 16, 2008; accepted August 12, 2008; published online September 9, 2008

Purpose. Determine the efficiency of cationic nanoparticles prepared by blending poly (lactide-*co*-glycolide; PLGA) and methacrylate copolymer (Eudragit® E100) to deliver a therapeutic gene encoding mouse interleukin-10, *in vitro* and *in vivo*.
Methods. Nanoparticles prepared with PLGA and E100 were evaluated for delivery of plasmid DNA encoding mouse interleukin-10 *in vitro* and *in vivo* in mice upon intramuscular injection. Blood-glucose, serum interferon-gamma levels and histology of pancreas were studied to determine therapeutic efficacy. Histological evaluation of skeletal muscle from the injection site was performed to assess the biocompatibility of nanoparticles.
Results. PLGA/E100 nanoparticles showed endosomal escape evidenced by confocal microscopy and buffering ability. Transfecting HEK293 cells with plasmid-loaded PLGA/E100 nanoparticles resulted in significantly ($p<0.05$) greater expression of interleukin-10 compared to PLGA nanoparticles. Mice treated with PLGA/E100 nanoparticles displayed higher serum levels of interleukin-10 and lower blood glucose levels compared to those treated with interleukin-10 plasmid alone or PLGA nanoparticles. High expression of interleukin-10 facilitated suppression of interferon-gamma levels and reduced islet infiltration. Histology of muscle showed that nanoparticles were biocompatible and did not cause chronic inflammatory response.
Conclusions. Nanoparticles prepared by blending PLGA with methacrylate can efficiently and safely deliver plasmid DNA encoding mouse interleukin-10 leading to prevention of autoimmune diabetes.

KEY WORDS: interferon-gamma (IFN-γ); interleukin-10 (IL-10); plasmid DNA; poly (lactide-*co*-glycolide) (PLGA); polymethacrylate.

INTRODUCTION

Intramuscular injection of plasmid DNA has been previously reported to result in sustained and detectable levels of expressed protein in the blood (1,2). Gene delivery to skeletal muscle is attractive due to its anatomical, physiological and cellular properties (3). Skeletal muscle has abundant vascular supply to transport expressed proteins into the blood circulation. Muscle fibers are post mitotic and do not divide normally providing a stable environment for transgene expression. When muscle fibers are damaged, they are quickly replaced by stem-like precursor cells, known as satellite cells. Major limitation for the clinical application of naked DNA is low levels of gene expression since very high DNA dose is required to elicit a therapeutic response.

Cationic polymers such as polyethyleneimine (PEI), polymethacrylates, poly-L-lysine (PLL), and chitosan form polyplexes by condensing pDNA into nanometer-size complexes (4–9). PEI has been used to deliver both plasmid DNA and antisense oligonucleotides through intramuscular route (10,11). PEI is partially protonated at physiologic pH and undergoes further protonation at endosomal pH causing endosomal destabilization (proton sponge effect) (12). Clinical potential of PEI may be limited since acute toxicity has been reported with the use of PEI both *in vitro* and *in vivo* (13,14). Polymethacrylates containing tertiary amine groups have displayed proton buffering ability similar to PEI with minimal toxicity (15). Polymethacrylates containing tertiary amine with different functional side groups have been synthesized and evaluated for gene delivery (16).

Type 1 diabetes is a chronic autoimmune disease resulting from selective destruction of pancreatic β-cells mediated by T lymphocytes leading to gradual reduction in body's ability to produce insulin (17,18). Interleukin-10 (IL-10), a pleiotropic cytokine produced primarily by Th2 cells, demonstrates potent anti-inflammatory activity via down regulation of the pro-inflammatory cytokines released by activated immune competent cells (19,20). However, the therapeutic application of IL-10 is severely limited by very short plasma half life (~2 min). This limitation can potentially be overcome by delivering a gene encoding IL-10 leading to endogenous production of IL-10. Studies have suggested that

[1] Department of Pharmaceutical Sciences, College of Pharmacy, Nursing, and Allied Sciences, North Dakota State University, Fargo, North Dakota 58105, USA.
[2] To whom correspondence should be addressed. (e-mail: Jagdish.Singh@ndsu.edu)

0724-8741/09/0100-0072/0 © 2008 Springer Science + Business Media, LLC

IL-10 gene delivery can result in suppression of autoimmune response caused by pro-inflammatory cytokines (21–24).

In the present study, we investigated the efficiency of cationic nanoparticles, prepared using a blend of poly (lactide-*co*-glycolide) (PLGA) and polymethacrylate, to deliver pDNA encoding mouse IL-10, *in vitro* and *in vivo*. Methacrylate copolymer Eudragit® E100 used in this study is a copolymer of *n*-butyl methacrylate, 2-dimethylaminoethyl methacrylate, and methyl methacrylate in a 1:2:1 ratio with an average molecular weight of 150 kDa. We hypothesized that nanoparticles prepared by blending PLGA with polymethacrylate using cationic surfactant cetyl trimethyl ammonium bromide (CTAB) will display positive zeta potential and high plasmid loading efficiency with greater expression of the transgene compared to PLGA nanoparticles. Confocal microscopy was used to study the cellular uptake and internalization of nanoparticles. Proton buffering ability of nanoparticles was evaluated by acid titrimetry. Expression of mouse interleukin-10 was observed *in vitro* and *in vivo*. The therapeutic effect of the expressed interleukin-10 in preventing autoimmune destruction of pancreatic beta cells (insulitis) was investigated *in vivo* in mice.

MATERIALS AND METHODS

Materials

The plasmids, pUMVC3mIL10 (encoding mouse interleukin-10), and pUMVC3 (blank), were generous gifts from Aldevron, LLC (Fargo, ND, USA). Poly (DL-lactide-*co*-glycolide; PLGA; inherent visc. 0.17 dL/g, MW≈10,000) was purchased from Birmingham Polymers, Inc. (Birmingham, AL, USA). Coumarin 6 was purchased from Polysciences Inc. (Warrington, PA, USA). Eudragit® E100 was a gift from Rohm Pharma (Weiterstadt, Germany). Cetyltrimethylammonium bromide (CTAB) was obtained from Sigma Chemical Company (St. Louis, MO, USA). Human embryonic kidney (HEK293) cell line was obtained from American Type Culture Collection (ATCC, Rockville, MD, USA). ELISA kits for the detection of mouse IL-10 and mouse IFN-γ were purchased from eBioscience (San Diego, CA, USA) and Biolegend (San Diego, CA, USA), respectively. De-ionized water was used to prepare all solutions and buffers.

Preparation and Characterization of Nanoparticles

Nanoparticles were prepared using W/O/W emulsion/solvent evaporation technique. Briefly, PLGA, either alone, or in combination with E100 (50% *w*/*w* total polymer), was dissolved in 10 ml dichloromethane (DCM) to yield total polymer concentration of 50 mg/ml. Phosphate buffered saline (PBS; 1 ml) was dispersed into the polymer solution by sonication at 80 W for 1 min using an ultrasonic homogenizer (Model 150 V/T, Biologics Inc., Manassas, VA, USA) to form a primary w/o emulsion. Primary emulsion was added to 50 ml aqueous solution of cetyltrimethylammonium bromide (CTAB; 0.5% *w*/*v*) and homogenized for 12 h at 4,000 rpm using a homogenizer (Model L4RT, Silverson, UK), leading to the formation of secondary w/o/w emulsion with subsequent evaporation of the organic phase. The nanoparticles were separated by centrifugation at 10,000 rpm and washed twice in order to remove excess surfactant. Finally, the particles were lyophilized for 24 h and stored at −20°C until further use.

Sizing of particles was done on a PSS/NICOMP 380 DLS particle sizing system (Santa Barbara, CA, USA). Sample dilution was done in distilled water (pH 6.8). Six sub-runs were used for each measurement. The zeta potential was measured on Zetasizer Nano ZS90 (Malvern Instruments, UK). A concentration of 0.1–0.5% *w*/*w* was chosen for the zeta potential measurements. The measurements were performed in 10 mM Phosphate Buffer (pH 7.4) using disposable zeta cells (DTS 1060) and the general purpose protocol at 27° C. A manual duration of about 30 sub-runs was used for each measurement. The mean zeta potential was determined using phase analysis light scattering technique. Plasmid loading was performed by suspending the nanoparticles in a solution of plasmid DNA at a theoretical loading of 10 μg/mg nanoparticles (1%) at 4°C for 6 h with shaking. The loaded particles were separated by centrifugation at 10,000 rpm, washed twice with distilled water, and finally lyophilized. Plasmid loading efficiency was determined by analyzing the supernatants at 260 nm.

Cellular Uptake of Nanoparticles

Cellular uptake and internalization of nanoparticles was studied by confocal microscopy in Human Embryonic Kidney (HEK293) cells. The cells were plated at a density of 2×10^5/chamber in Lab-Tek™ II Chamber Slide™ System (Nalge Nunc International). Fluorescent molecule (coumarin 6) was encapsulated inside nanoparticles during primary emulsification. The fluorescent-labeled nanoparticles were incubated with cells for different time points. Thereafter, the cells were washed with PBS, fixed in 4% paraformaldehyde, mounted on the Chamber Slide and cover slipped. The slides were observed under confocal microscope (Olympus FV300) using multi-line argon laser (458 nm) and images were captured using Fluoview™ software.

Buffering Ability of Nanoparticles

The buffering ability of nanoparticles was determined by titrimetric assay according to the method reported previously (25), with slight modifications. Briefly, the nanoparticles were suspended at a concentration of 10 mg/ml in a 150 mM NaCl. The pH of the solution was adjusted to 9. The suspension was kept under stirring and was titrated with small increments of 0.1 N HCl (10 μl) until a pH of 3 was achieved. The slope of the titration curve provides an indication of the buffering ability of nanoparticles.

Expression of Interleukin-10 *In Vitro*

In vitro expression of IL-10 was studied in HEK293 cells at 24, 48, and 72 h post transfection. The cells were maintained in modified Minimum Essential Medium (Eagle; EMEM) supplemented with 10% fetal bovine serum (FBS) in 5% CO_2 incubator at 37°C. Cells were plated in 24-well plates at 2×10^5 cells/well. Nanoparticles were added at a dose equivalent to 500 ng/well pDNA in complete serum medium. After incubation for different durations, the cells were washed and lysed. The quantity of IL-10 in cell lysate was

measured by Enzyme-Linked ImmunoSorbent Assay (ELISA) according to manufacturer's protocol.

Animals

Male BALB/c mice, 5–6 week old, were obtained from Ace Animals, Inc. (Boyertown, PA, USA). Animals were provided rodent food and water *ad libitum*. The experiments were conducted in accordance with the guidelines of the Institutional Animal Care and Use Committee (IACUC) at NDSU and "Principles of Laboratory Animal Care" (NIH publication #85-23, revised in 1985). Insulitis was induced in mice with multiple low doses of streptozotocin (STZ). Briefly, STZ was reconstituted in citrate buffer (pH 4.5) and injected intraperitoneally within 5 min of preparation at a dose of 40 mg/kg body weight for five consecutive days. The STZ-treated animals were divided into different treatment groups (six animals per group). Control group ($n=6$) was treated with citrate buffer instead of STZ.

Intramuscular Delivery of Plasmid DNA in Mice

Plasmid encoding mouse IL-10 (pUMVC3mIL10) was injected into right tibialis anterior (TA) muscle of STZ treated mice, either passively or loaded on PLGA or PLGA/E100 nanoparticles, at a dose of 50 μg, on the day of first STZ injection. Two groups received blank plasmid (pUMVC3) loaded on PLGA and PLGA/E100 nanoparticles, respectively, along with STZ treatment as a negative control for IL-10 plasmid. One group was left untreated after STZ injections. Blood samples were taken at weekly intervals for six consecutive weeks from animals through submandibular bleeding. Blood glucose levels were measurement by glucose oxidase method using Glucometer Elite (Bayer).

Determination of Interleukin-10 and Interferon-Gamma Levels in Serum

Serum concentrations of IL-10 and IFN-γ were determined by ELISA. Weekly blood samples were collected by submandibular bleeding and allowed to clot for 30 min. Sera were separated by centrifugation at 1,500 rpm for 7 min at 4°C and stored at −80°C until further analysis. Concentrations of IL-10 and IFN-γ were determined by ELISA according to manufacturer's protocols.

Histological Evaluation

At the end of 6 weeks, the animals were euthanized for histological studies. Pancreas was removed, fixed in 10% neutral buffered formalin, and embedded in paraffin. Six-μm thick sections were cut and stained with hematoxylin–eosin and observed under light microscope. Morphology of the pancreas was studied to determine the therapeutic efficacy of expressed IL-10 in suppressing autoimmune insulitis by preventing the infiltration of lymphocytes and neutrophils into the islets.

In order to study the biocompatibility of PLGA/E100 nanoparticles, animals were euthanized at predetermined time points post-injection and Tibialis Anterior (TA) muscles were removed and processed for histological studies. The TA muscles slides were observed under light microscope for the presence of chronic inflammation, fibrosis, and necrosis.

Statistical Analysis

The results were expressed as mean±standard deviation ($n=6$). Statistical comparisons were made using one-way analysis of variance and student's unpaired t-test; $p<0.05$ was considered significant.

RESULTS

Characterization of Cationic Nanoparticles

PLGA and PLGA/E100 nanoparticles showed similar mean particles sizes (~800 nm) and polydispersity indices (~0.2). The zeta potentials of PLGA and PLGA/E100 nanoparticles were 4.2±0.7 mV and 58.5±2.1 mV, respectively, before plasmid loading, and 1.9±0.2 mV and 42.7±1.1 mV, respectively, after plasmid loading. Both formulations displayed plasmid loading in excess of 8.5 μg/mg (85% of theoretical loading) nanoparticles.

Cellular Internalization of Cationic Nanoparticles

Cellular internalization of nanoparticles was observed by confocal laser scanning microscope (CLSM) 12 h, and 24 h post-treatment (Fig. 1). We specifically wanted to study the effect of addition of E100 on endosomal escape of nanoparticles (proton sponge). Cellular uptake and internalization of PLGA/E100 nanoparticles was compared with PLGA nanoparticles using fluorescent molecule coumarin 6. At 12 h post-treatment, the cells treated with PLGA nanoparticles showed presence of intact, bright fluorescent particles with no diffused fluorescence in the cytoplasm. Cells treated with PLGA/E100 nanoparticles on the other hand showed significant amount of diffused fluorescence indicating that the particles were able to escape the endosomal compartments and release their payload into the cytoplasm. Even at 24 h post-treatment, cells treated with PLGA nanoparticles showed presence of intact particles which may be either associated with the cell surface or inside the endosome. Cells treated with PLGA/E100 particles showed intense fluorescence evenly distributed within the cytoplasm with no visible presence of intact particles. These results suggest that E100 may confer endosomal buffering ability to the nanoparticles causing increased endosomal escape, and subsequently greater transfection efficiency as compared to particles prepared without E100.

Buffering Ability of Nanoparticles

Endosomal buffering ability of nanoparticles was confirmed by titrimetric assay. The changes in pH due to gradual addition of 0.1 N HCl to the nanoparticle suspension were determined for PLGA and PLGA/E100 formulations (Fig. 2). Particles containing E100 showed a greater resistance to drop in the pH compared to PLGA nanoparticles without E100 suggesting that E100 imparts buffering ability to nanoparticles. Greater buffering ability of PLGA/E100 nanoparticles may be responsible for faster and higher endosomal escape of nanoparticles as seen in CLSM studies.

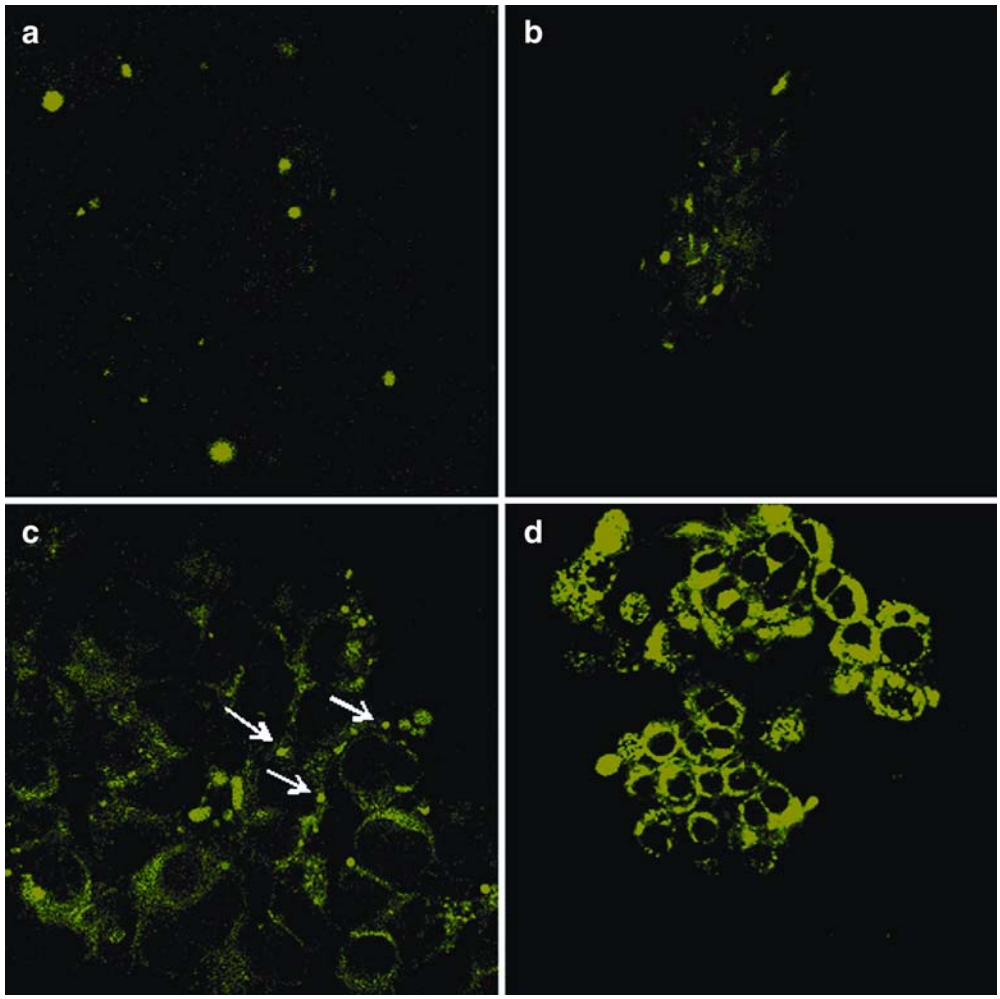

Fig. 1. Confocal laser scanning microscopic images of the uptake of PLGA (**A**, **C**), and PLGA/E100 (**B**, **D**) nanoparticles in HEK293 cells, 12 h (**A**, **B**), and 24 h (**C**, **D**) post-treatment. Diffused fluorescence in the cytoplasm suggests escape of nanoparticles from the endosomal compartment. Arrows indicate presence of intact particles.

Expression of Interleukin-10 *In Vitro*

In vitro transfection efficiency of cationic nanoparticles was determined by measuring the expression of IL-10 plasmid in HEK293 cells (Fig. 3). Expression of IL-10 was measured at 24, 48, and 72 h post-transfection by ELISA according to the manufacturer's protocol. The expression of IL-10 was significantly greater ($p<0.05$) for PLGA/E100 nanoparticles compared to PLGA nanoparticles at all the time points. Expression of IL-10 for PLGA/E100 in comparison to

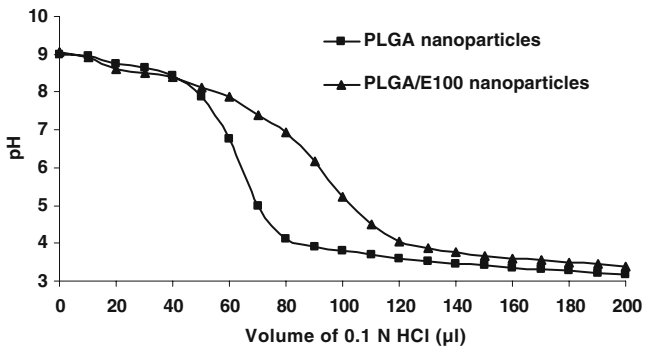

Fig. 2. Buffering ability of cationic nanoparticles determined by acid titration with 0.1 N HCl. An increase in the buffering ability of nanoparticles was observed in the presence of E100 in the formulation.

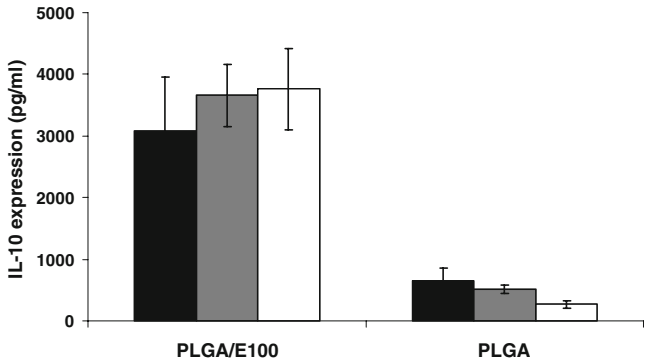

Fig. 3. Expression of interleukin-10 in HEK293 cells. Cells were treated with nanoparticle formulations at a dose equivalent to 500 ng/well pDNA for 24 h (*black*), 48 h (*grey*), and 72 h (*white*). Quantity of IL-10 was measured in cell lysate by ELISA. Mean±SD ($n=4$) is presented.

PLGA nanoparticles varied from 4.7-fold at 24 h to 13.8-fold at 72 h.

Determination of Blood Glucose Levels in Mice

Blood glucose levels measured at weekly interval using glucose oxidase method are presented in Fig. 4. Animals receiving STZ treatment showed a significant rise ($p<0.05$) in blood glucose compared to the control animals starting at three weeks post-treatment. Likewise, the animals treated with blank pDNA loaded on PLGA and PLGA/E100 nanoparticles showed significantly ($p<0.05$) elevated blood glucose levels at 3 and 4-weeks post-treatment, respectively. Increase in the blood glucose level in these animals can be attributed to increased insulitis due to streptozotocin treatment. Groups receiving IL-10 plasmid passively or loaded on PLGA nanoparticles showed a significant ($p<0.05$) increase in blood glucose 6 weeks after the injection. Blood glucose concentration of group receiving IL-10 plasmid loaded on PLGA/E100 nanoparticles was similar to control untreated animals at all time points.

Determination of Serum IL-10 and IFN-γ Levels in Mice

Serum levels of IL-10 and IFN-γ measured each week by ELISA are presented in Figs. 5 and 6, respectively. IL-10 levels for the STZ-treated animals remained similar to control animals at all the time points. Mice receiving IL-10 plasmid passively showed higher levels of serum IL-10 for the first 2 weeks. However, the concentration of IL-10 dropped back to the normal (control) levels at 3 weeks. In animals receiving IL-10 plasmid loaded on PLGA nanoparticles, the concentration of IL-10 was higher compared to passive delivery after the first week and was sustained over the duration of the study. Higher expression of IL-10, however, was observed for animals treated with IL-10 plasmid loaded on PLGA/E100 nanoparticles. Serum concentration of IL-10 in these animals was significantly ($p<0.05$) elevated at all time points as compared to passive delivery and for first 2 weeks as compared to PLGA+IL-10 group.

All groups except the control and passive delivery showed significant ($p<0.05$) increase in levels of IFN-γ in the serum 1 week post-treatment. In animals treated with IL-10 plasmid loaded on nanoparticles, the IFN-γ levels dropped to normal levels by second week. A temporary increase in the levels of IFN-γ can be attributed to the acute inflammatory response to the nanoparticles and injury due to the needle. For groups receiving STZ alone or blank pDNA with nanoparticles, the levels of IFN-γ were significantly ($p<0.05$) higher compared to control throughout the duration of the study.

Histological Analysis

At the end of 6-week study, the animals were euthanized and pancreas was excised for histological examination. Pancreatic sections were observed under light microscope for immune infiltration. Pancreatic islets of animals after different treatments were compared to those of untreated control animals (Fig. 7). Pancreas of STZ-treated animals showed severe immune infiltration in the islets. Pancreas of animals treated with passive IL-10 showed much reduced inflammation of islets compared to STZ group. However, some infiltration was also observed for passive pDNA and PLGA nanoparticles-treated animals. Animals treated with PLGA/E100 nanoparticles on the other hand, showed similar islet morphology to that of the control animals. The pancreatic islets of these animals were intact and showed no signs of insulitis.

In vivo biocompatibility of PLGA/E100 nanoparticles containing IL-10 plasmid was evaluated by studying the histology of tibialis anterior (TA) muscle (Fig. 8). Animals were euthanized at predetermined time points and the TA muscles that received the injection were excised. Histological examination was performed under light microscope after hematoxylin–eosin staining. Muscle samples taken 1-week

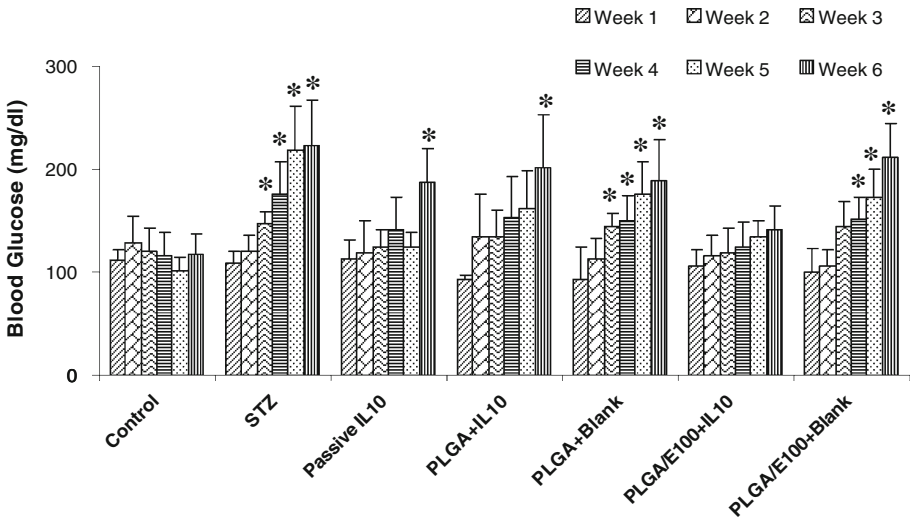

Fig. 4. Blood glucose levels of mice at different time points post treatment ($n=6$). Blood glucose levels were determined at weekly time points by glucose oxidase method. A * indicates that the values are statistically greater than control group at that time point as determined by *t*-test ($p<0.05$).

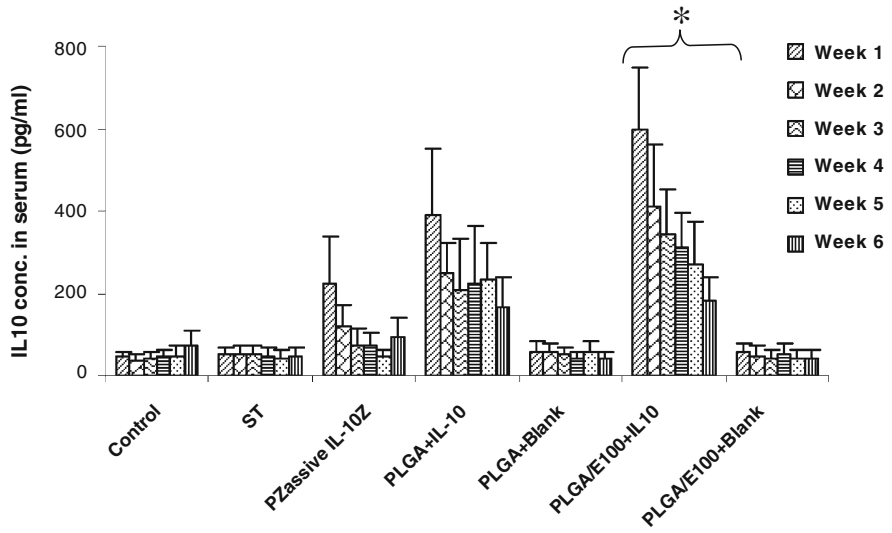

Fig. 5. Concentration of interleukin-10 in serum at different time points post-treatment (n=6). Serum samples were taken at weekly intervals and interleukin-10 concentration was determined by ELISA. A * indicates that the values are statistically greater than passive delivery group at that time point as determined by t-test ($p<0.05$).

post treatment showed extensive infiltration of lymphocytes and macrophages along with damage to the muscle fibers. However, the inflammation seemed to reduce considerably 2-week after treatment. After 6-week, the histology of muscles receiving nanoparticles was comparable to the muscle from the control animals.

DISCUSSION

Cationic polymers have invoked interest due to their ability to condense polyanionic DNA and facilitate cellular internalization. In this study, cationic nanoparticles prepared by combining PLGA and Eudragit® E 100 were evaluated for delivery of a therapeutic plasmid through intramuscular route. The effect of formulation variables such as polymer ratios and surfactant concentration on size, shape, plasmid loading, zeta potential, and *in vitro* transfection efficiency have been studied previously in our lab. Cationic surfactant, CTAB, was used in order to increase the zeta potential of the PLGA/E100 nanoparticles. Loading of plasmid DNA on the surface of nanoparticles is attractive due to potential advantages such as faster and more complete release, protection of polynucleotides from denaturing conditions during formulation, and additional adjuvant effect for DNA vaccines (26,27).

Proton buffering ability of cationic polymers is believed to have an impact on the transfection efficiency by facilitating endosomal destabilization (Proton sponge) (12). This property was investigated using confocal microscopy and titrimetric assay. As expected PLGA/E100 particles were able to release the fluorescent molecule, coumarin 6, in the cyto-

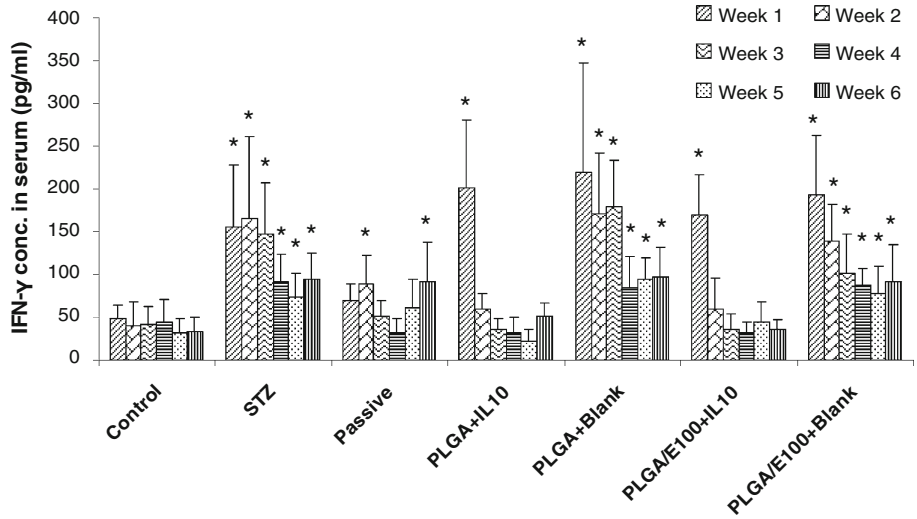

Fig. 6. Concentration of interferon-gamma in serum at different time points post-treatment (n=6). Serum samples were taken at weekly intervals and interferon-gamma concentration was determined by ELISA. A * indicates that the values are statistically greater than control group at that time point as determined by t-test ($p<0.05$).

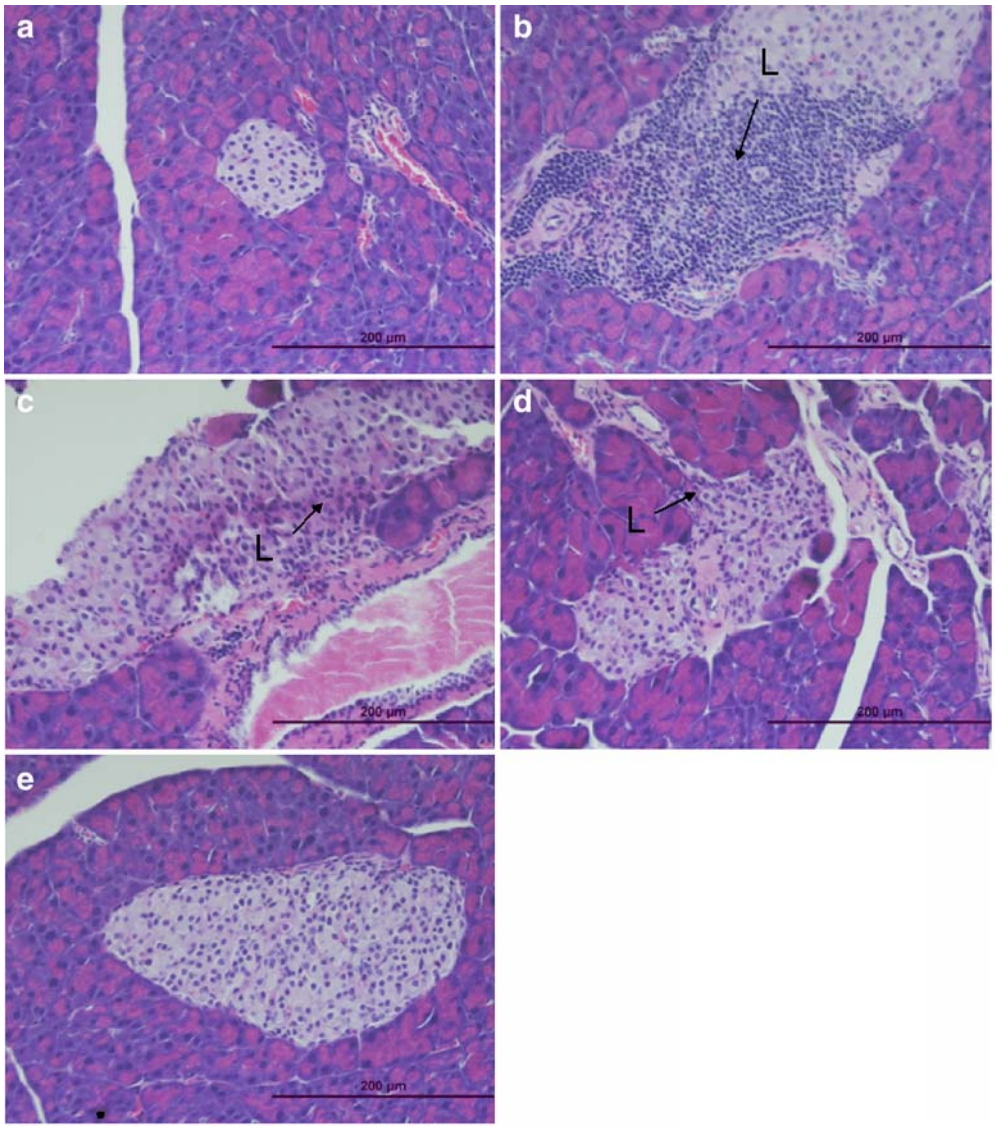

Fig. 7. Histology of pancreas of control animal (**A**); and animals treated with STZ (**B**), passive pDNA (**C**), PLGA nanoparticles (**D**), and PLGA/E100 nanoparticles (**E**) 6-week post-treatment. Intense inflammation due to lymphocytes (*L*) was observed in the pancreas of STZ-treated animals. Mild inflammation was also observed for passive delivery and PLGA nanoparticles-treated animals. The morphology of pancreas from PLGA/E100 nanoparticle treated group was similar to that of control pancreas.

plasm to a much greater degree as compared to PLGA nanoparticles. There may not be a difference in cellular uptake of these formulations; however, the processing of particles post-internalization is likely to be different. Plasmid DNA loaded onto PLGA nanoparticles is more likely to be degraded by lysosomal nucleases due to lack of endosomal buffering ability of the delivery system. Since protein expression is dictated by the amount of DNA reaching the nuclei of the cells, ability of nanoparticles to escape endosomal compartment assumes great significance. Cells treated with PLGA nanoparticles showed large number of intact particles even 24 h post-treatment which indicates that these particles were either associated with cell surface or inside the endosomal compartment. An increase in buffering ability at endosomal pH was observed in the presence of E100 which confirms that PLGA/E100 nanoparticles possess the potential to destabilize the endosomes.

In vitro studies using Interleukin-10 plasmid showed that the transfection with PLGA/E100 nanoparticles led to higher expression of IL-10 compared to PLGA nanoparticles. This could be due to faster endosomal escape of PLGA/E100 nanoparticles because of proton buffering ability of the cationic polymer, E100. Thus, the difference in transfection efficiencies of the two formulations is likely to be due to the difference in their processing in the endosome after uptake.

Although the exact etiology of type-1 diabetes is unknown, infiltration of autoreactive immune cells into the pancreatic islets leading to selective destruction of pancreatic beta cells is believed to be the reason for type 1 diabetes (28). This process is enhanced by proinflammatory cytokines secreted from Th1 $CD4^+$ cells such as IFN-γ and IL-2. Previous studies have shown that delivering gene encoding Th2 cytokines such as IL-4 and IL-10 can lead to suppression of autoimmune response against pancreatic beta cells.

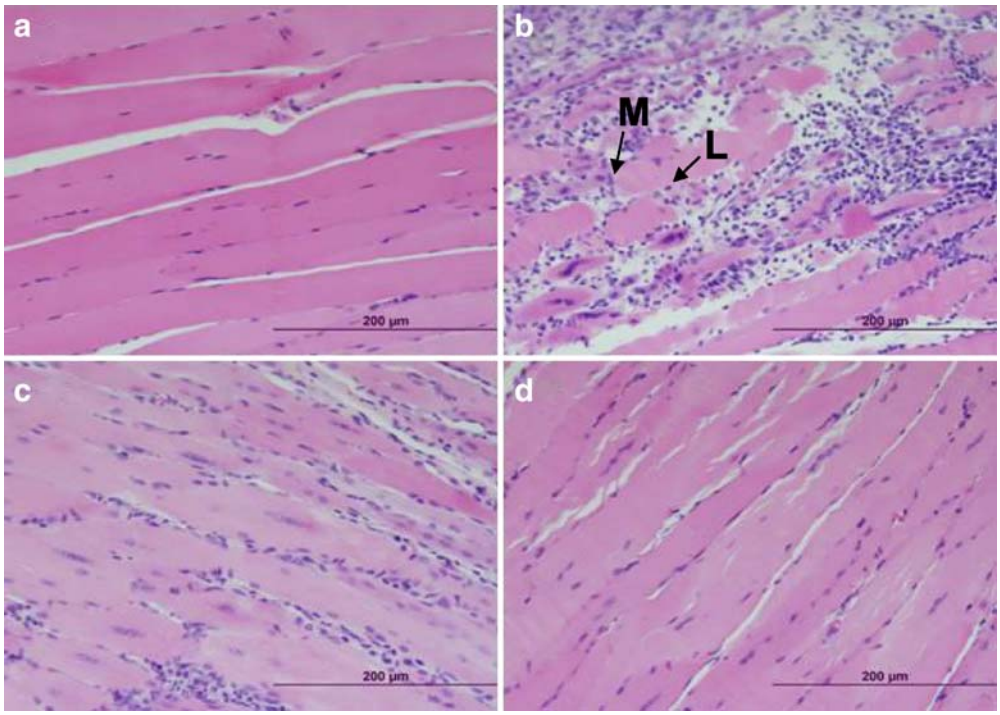

Fig. 8. Histology of TA muscle from control animal (**A**); and animals treated with PLGA/E100 nanoparticles, 1-week (**B**), 2-week (**C**), and 6-week (**D**) post-treatment. Inflammation due to lymphocytes *L*) and macrophages (*M*) was observed, 1 week post-treatment.

Multiple low-dose STZ treatment is a well established treatment for induction of autoimmune response against pancreatic beta cells in mice. Therapeutic effect of IL-10 gene delivery was studied by measuring blood glucose levels. Animals treated with STZ showed significantly elevated blood glucose 3-week post treatment. In case of animals treated with PLGA/E100 nanoparticles containing IL-10 gene, the blood glucose levels were not different from control untreated animals throughout the study. Blood glucose levels were lower in animals treated with PLGA/E100 nanoparticles compared to those treated with PLGA nanoparticles or IL-10 plasmid passively.

Increase in the concentration of IL-10 at 1 week after treatment was observed for all the groups treated with IL-10 plasmid. An increase in the IL-10 concentration was transient in animals treated with pDNA passively. The IL-10 levels in passive delivery group dropped back to the normal physiologic levels at the end of 3 weeks. Transient expression of IL-10 for 2 weeks in mice after delivery of naked DNA has been reported (29). Transient expression may entail repeated administration and thus decreased patient compliance. Therefore, it is highly desirable that the delivery system is efficient and provides sustained expression of the therapeutic protein. Nanoparticulate delivery systems show great promise towards achievement of this goal. There was a significant ($p<0.05$) increase in the concentration of IL-10 in animals treated with IL-10 plasmid loaded on PLGA/E100 nanoparticles in comparison to passive delivery of the plasmid. Although there was a drop in expression at later time points, the concentration was sustained above physiologic levels over the duration of study. The loss of expression over time may be due to deactivation of the promoter or the turnover of muscle fibers.

The IFN-γ levels were measured on a weekly basis to assess the inhibitory effect of the expressed IL-10 towards pro-inflammatory cytokines. IFN-γ exhibits potent pro-inflammatory effect through activation of macrophages and T cells leading to the destruction of pancreatic beta cells (30). Although IFN-γ has not been shown to be singularly responsible for Type 1 diabetes, disruption of the IFN-γ gene has resulted in delay in diabetes onset (31). Results revealed that IFN-γ was upregulated in animals treated with STZ alone. Upregulation of IFN-γ is due to the autoimmune response initiated by low-dose STZ treatment. An increase in the concentration of IFN-γ leads to recruitment of T cells and macrophages into the pancreas resulting in an increased inflammation. These inflammatory cells in turn secrete more IFN-γ causing further recruitment of cells which leads to destruction of pancreatic beta cells. Inhibition of IFN-γ production by IL-10 may result in reduced inflammation and enhanced protection of beta cells from destruction. An increased level of IFN-γ in serum found at 1 week post-treatment is likely to be due to the inflammatory response to the needle injury as well as acute immune response to the nanoparticle formulation. In all the animals receiving IL-10 plasmid, the levels of IFN-γ decreased in subsequent weeks due to the inhibitory effect of the expressed IL-10 on IFN-γ production. Animals treated with IL-10 plasmid passively displayed an increase in IFN-γ levels at later time points possibly due to the decline in IL-10 levels. Sustained inhibition of IFN-γ was observed for animals treated with PLGA/E100 nanoparticles throughout the duration of study.

Histological section revealed that the islets of animals receiving only STZ treatment were severely infiltrated. Treatment with IL-10 plasmid did exhibit a protective effect on the pancreas. The protective effect seemed to be related

with extent and longevity of expression of IL-10 in animals. Therefore, although the inflammation of the pancreas was markedly reduced in animals treated with IL-10 plasmid passively and loaded on PLGA nanoparticles, it was not sufficient to completely protect the pancreas. On the other hand treatment with PLGA/E100 nanoparticles loaded with IL-10 plasmid completely preserved the morphology of pancreatic islets possibly due to higher and more sustained expression of IL-10.

Histology of the skeletal muscle was studied after injection of PLGA/E100 nanoparticles since cationic polymers have been reported to cause severe immune response. We did observe an acute inflammatory response with infiltration of macrophages and lymphocytes. The transient inflammation can be due to a combination of acute inflammatory response to the nanoparticles and tissue injury caused by the needle. However, the inflammation regressed at later time points. The morphology of the tissue receiving nanoparticles injection was similar to the control untreated tissue suggesting that the nanoparticles were biocompatible upon intramuscular injection and did not cause chronic inflammatory response.

CONCLUSION

The potential of PLGA/E100 cationic nanoparticles to deliver a therapeutic gene *in vitro* and *in vivo* was investigated. PLGA/E100 nanoparticles increased the expression of IL-10 compared to PLGA nanoparticles *in vitro*. Intramuscular delivery of PLGA/E100 nanoparticles loaded with IL-10 plasmid led to increased expression of IL-10 which resulted in effective protection against insulitis. Histological studies showed that the nanoparticles did not lead to chronic inflammation. Our results suggest the feasibility of using cationic PLGA/E100 nanoparticles for IL-10 gene delivery for the prevention of autoimmune diabetes.

ACKNOWLEDGEMENTS

We acknowledge financial support to JS from NIH grant # HD 46483-01 and Fraternal Order of Eagles fund.

REFERENCES

1. J. A. Wolff, R.W. Malone, P. Williams, W. Chong, G. Acsadi, A. Jani, and P. L. Felgner. Direct gene transfer into mouse muscle *in vivo*. *Science* **247**:1465–1468 (1990). doi:10.1126/science.1690918.
2. S. K. Tripathy, E. C. Svensson, H. B. Black, E. Goldwasser, M. Margalith, P. M. Hobart, and J. M. Leiden. Long-term expression of erythropoietin in the systemic circulation of mice after intramuscular injection of a plasmid DNA vector. *Proc. Natl. Acad. Sci. U. S. A.* **93**:10876–10880 (1996). doi:10.1073/pnas.93.20.10876.
3. Q. L. Lu, G. Bou-Gharios, and T. A. Partridge. Non-viral gene delivery in skeletal muscle: a protein factory. *Gene. Ther.* **10**:131–142 (2003). doi:10.1038/sj.gt.3301874.
4. I. S. Kim, S. K. Lee, Y. M. Park, Y. B. Lee, S. C. Shin, K. C. Lee, and I. J. Oh. Physicochemical characterization of poly(L-lactic acid) and poly(D,L-lactide-*co*-glycolide) nanoparticles with polyethylenimine as gene delivery carrier. *Int. J. Pharm.* **298**:255–262 (2005). doi:10.1016/j.ijpharm.2005.04.017.
5. P. Li, J. M. Zhu, P. Sunintaboon, and F. W. Harris. New route to amphiphilic core-shell polymer nanospheres: graft copolymerization of methyl methacrylate from water-soluble polymer chains containing amino groups. *Langmuir* **18**:8641–8646 (2002). doi:10.1021/la0261343.
6. D. Y. Kwoh, C. C. Coffin, C. P. Lollo, J. Jovenal, M. G. Banaszczyk, P. Mullen, A. Phillips, A. Amini, J. Fabrycki, R. M. Bartholomew, S. W. Brostoff, and D. J. Carlo. Stabilization of poly-L-lysine/DNA polyplexes for *in vivo* gene delivery to the liver. *Biochim. Biophys. Acta.* **1444**:171–190 (1999).
7. R. Moriguchi, K. Kogure, H. Akita, S. Futaki, M. Miyagishi, K. Taira, and H. Harashima. A multifunctional envelope-type nano device for novel gene delivery of siRNA plasmids. *Int. J. Pharm.* **301**:277–285 (2005). doi:10.1016/j.ijpharm.2005.05.021.
8. A. Bozkir and O. M. Saka. Chitosan nanoparticles for plasmid DNA delivery: effect of chitosan molecular structure on formulation and release characteristics. *Drug Deliv.* **11**:107–112 (2004). doi:10.1080/10717540490280705.
9. K. A. Howard, U. L. Rahbek, X. Liu, C. K. Damgaard, S. Z. Glud, M. Ø. Andersen, M. B. Hovgaard, A. Schmitz, J. R. Nyengaard, F. Besenbacher, and J. Kjems. RNA interference *in vitro* and *in vivo* using a novel chitosan/siRNA nanoparticle system. *Mol. Ther.* **14**:476–484 (2006). doi:10.1016/j.ymthe.2006.04.010.
10. S. Wang, N. Ma, S. J. Gao, H. Yu, and K. W. Leong. Transgene expression in the brain stem effected by intramuscular injection of polyethylenimine/DNA complexes. *Mol. Ther.* **3**:658–664 (2001). doi:10.1006/mthe.2001.0324.
11. J. H. Williams, S. R. Sirsi, D. R. Latta, and G. J. Lutz. Induction of dystrophin expression by exon skipping in mdx mice following intramuscular injection of antisense oligonucleotides complexed with PEG-PEI copolymers. *Mol. Ther.* **14**:88–96 (2006). doi:10.1016/j.ymthe.2005.11.025.
12. J. P. Behr. The proton sponge—a trick to enter cells the viruses did not exploit. *CHIMIA* **51**:34–36 (1997).
13. P. Chollet, M. C. Favrot, A. Hurbin, and J. L. Coll. Side-effects of a systemic injection of linear polyethylenimine–DNA complexes. *J. Gene. Med.* **4**:84–91 (2002). doi:10.1002/jgm.237.
14. S. M. Moghimi, P. Symonds, J. C. Murray, A. C. Hunter, G. Debska, and A. Szewczyk. A two-stage poly(ethylenimine)-mediated cytotoxicity: implications for gene transfer/therapy. *Mol. Ther.* **11**:990–995 (2005). doi:10.1016/j.ymthe.2005.02.010.
15. P. Dubruel, B. Christiaens, M. Rosseneu, J. Vandekerckhove, J. Grooten, V. Goossens, and E. Schacht. Buffering properties of cationic polymethacrylates are not the only key to successful gene delivery. *Biomacromolecules* **5**:379–388 (2004). doi:10.1021/bm034438d.
16. P. Dubruel, B. Christiaens, B. Vanloo, K. Bracke, M. Rosseneu, J. Vandekerckhove, and E. Schacht. Physicochemical and biological evaluation of cationic polymethacrylates as vectors for gene delivery. *Eur. J. Pharm. Sci.* **18**:211–220 (2003). doi:10.1016/S0928-0987(02)00280-4.
17. J. W. Yoon and H. S. Jun. Autoimmune destruction of pancreatic beta cells. *Am. J. Ther.* **12**:580–591 (2005). doi:10.1097/01.mjt.0000178767.67857.63.
18. D. Mathis, L. Vence, and C. Benoist. Beta-Cell death during progression to diabetes. *Nature* **414**:792–798 (2001). doi:10.1038/414792a.
19. C. J. Clarke, A. Hales, A. Hunt, and B. M. Foxwell. IL-10-mediated suppression of TNF-alpha production is independent of its ability to inhibit NF kappa B activity. *Eur. J. Immunol.* **28**:1719–1726 (1998). doi:10.1002/(SICI)1521-4141(199805)28:05<1719::AID-IMMU1719>3.0.CO;2-Q.
20. T. A. Hamilton, Y. Ohmori, and J. Tebo. Regulation of chemokine expression by antiinflammatory cytokines. *Immunol. Res.* **25**:229–245 (2002). doi:10.1385/IR:25:3:229.
21. Z. L. Zhang, S. X. Shen, B. Lin, L. Y. Yu, L. H. Zhu, W. P. Wang, F. H. Luo, and L. H. Guo. Intramuscular injection of interleukin-10 plasmid DNA prevented autoimmune diabetes in mice. *Acta. Pharmacol. Sin.* **24**:751–756 (2003)Medline.
22. M. Lee, K. S. Ko, S. Oh, and S. W. Kim. Prevention of autoimmune insulitis by delivery of a chimeric plasmid encoding interleukin-4 and interleukin-10. *J. Control Release* **88**:333–342 (2003). doi:10.1016/S0168-3659(03)00031-2.

23. J. J. Koh, K. S. Ko, M. Lee, S. Han, J. S. Park, and S. W. Kim. Degradable polymeric carrier for the delivery of IL-10 plasmid DNA to prevent autoimmune insulitis of NOD mice. *Gene Ther.* **7**:2099–2104 (2000). doi:10.1038/sj.gt.3301334.
24. K. S. Ko, M. Lee, J. J. Koh, and S. W. Kim. Combined administration of plasmids encoding IL-4 and IL-10 prevents the development of autoimmune diabetes in nonobese diabetic mice. *Mol. Ther.* **4**:313–316 (2001). doi:10.1006/mthe.2001.0459.
25. M. X. Tang and F. C. Szoka. The influence of polymer structure on the interactions of cationic polymers with DNA and morphology of the resulting complexes. *Gene Ther.* **4**:823–832 (1997). doi:10.1038/sj.gt.3300454.
26. C. G. Oster, N. Kim, L. Grode, L. Barbu-Tudoran, A. K. Schaper, S. H. Kaufmann, and T. Kissel. Cationic microparticles consisting of poly(lactide-*co*-glycolide) and polyethylenimine as carriers systems for parental DNA vaccination. *J. Control Release.* **104**:359–377 (2005).
27. M. Singh, M. Briones, G. Ott, and D. O'Hagan. Cationic microparticles: a potent delivery system for DNA vaccines. *Proc. Natl. Acad. Sci. U. S. A.* **97**:811–816 (2000). doi:10.1073/pnas.97.2.811.
28. E. Kawasaki, N. Abiru, and K. Eguchi. Prevention of type 1 diabetes: from the view point of beta cell damage. *Diabetes Res. Clin. Pract.* **66**(Suppl 1):S27–32 (2004). doi:10.1016/j.diabres.2003.09.015.
29. V. Deleuze, D. Scherman, and M. F. Bureau. Interleukin-10 expression after intramuscular DNA electrotransfer: kinetic studies. *Biochem. Biophys. Res. Commun.* **299**:29–34 (2002). doi:10.1016/S0006-291X(02)02580-9.
30. B. Wang, I. André, A. Gonzalez, J. D. Katz, M. Aguet, C. Benoist, and D. Mathis. Interferon-gamma impacts at multiple points during the progression of autoimmune diabetes. *Proc. Natl. Acad. Sci. U. S. A.* **94**:13844–13849 (1997). doi:10.1073/pnas.94.25.13844.
31. B. Hultgren, X. Huang, N. Dybdal, and T. A. Stewart. Genetic absence of gamma-interferon delays but does not prevent diabetes in NOD mice. *Diabetes* **45**:812–817 (1996). doi:10.2337/diabetes.45.6.812.